Genetic Analyses of Conserved Residues in the Carboxyl-Terminal Domain of Human Immunodeficiency Virus Type 1 Integrase

The Harvard community has made this article openly available. Please share how this access benefits you. Your story matters

Citation	Lu, R., H. Z. Ghory, and A. Engelman. 2005. "Genetic Analyses of Conserved Residues in the Carboxyl-Terminal Domain of Human Immunodeficiency Virus Type 1 Integrase." Journal of Virology 79 (16): 10356–68. https://doi.org/10.1128/jvi.79.16.10356-10368.2005.
Citable link	http://nrs.harvard.edu/urn-3:HUL.InstRepos:41482902
Terms of Use	This article was downloaded from Harvard University's DASH repository, and is made available under the terms and conditions applicable to Other Posted Material, as set forth at http://nrs.harvard.edu/urn-3:HUL.InstRepos:dash.current.terms-of-use#LAA

JOURNAL OF VIROLOGY, Aug. 2005, p. 10356–10368 Vol. 79, No. 16
0022-538X/05/$08.00+0 doi:10.1128/JVI.79.16.10356–10368.2005

Genetic Analyses of Conserved Residues in the Carboxyl-Terminal Domain of Human Immunodeficiency Virus Type 1 Integrase

Richard Lu, Hina Z. Ghory, and Alan Engelman*

Department of Cancer Immunology and AIDS, Dana-Farber Cancer Institute, and Department of Pathology, Harvard Medical School, Boston, Massachusetts 02115

Received 1 February 2005/Accepted 2 May 2005

Results of in vitro assays identified residues in the C-terminal domain (CTD) of human immunodeficiency virus type 1 (HIV-1) integrase (IN) important for IN-IN and IN-DNA interactions, but the potential roles of these residues in virus replication were mostly unknown. Sixteen CTD residues were targeted here, generating 24 mutant viruses. Replication-defective mutants were typed as class I (blocked at integration) or class II (additional reverse transcription and/or assembly defects). Most defective viruses (15 of 17) displayed reverse transcription defects. In contrast, replication-defective HIV-1_{E246K} synthesized near-normal cDNA levels but processing of $Pr55^{gag}$ was largely inhibited in virus-producing cells. Because single-round HIV-$1_{E246K.Luc(R-)}$ transduced cells at approximately 8% of the wild-type level, we concluded that the late-stage processing defect contributed significantly to the overall replication defect of HIV-1_{E246K}. Results of complementation assays revealed that the CTD could function in *trans* to the catalytic core domain (CCD) in in vitro assays, and we since determined that certain class I and class II mutants defined a novel genetic complementation group that functioned in cells independently of IN domain boundaries. Seven of eight novel Vpr-IN mutant proteins efficiently *trans*-complemented class I active-site mutant virus, demonstrating catalytically active CTD mutant proteins during infection. Because most of these mutants inefficiently complemented a class II CCD mutant virus, the majority of CTD mutants were likely more defective for interactions with cellular and/or viral components that affected reverse transcription and/or preintegration trafficking than the catalytic activity of the IN enzyme.

Retrovirus replication is dependent on the integration of the reverse-transcribed viral genome into a host chromosome. Subsequent to target cell entry, the double-stranded DNA substrate for integration is generated by the viral enzyme reverse transcriptase (RT) upon conversion of the genomic RNA into DNA. Acting on the attachment (*att*) sites at the cDNA ends, the viral DNA recombinase or integrase (IN) catalyzes two distinct endonucleolytic reactions. For the first reaction, 3′ processing, human immunodeficiency virus type 1 (HIV-1) IN removes the dinucleotide GT from each end. This exposes a 3′ hydroxyl moiety in preparation for the second reaction, DNA strand transfer. Upon recognition and binding to a suitable target site, IN uses the 3′-OHs to cut the chromosome in a staggered fashion, which at the same time joins the viral ends to the 5′-phosphates of the cut. Cellular enzymes are likely involved in the repair of the resultant gapped product, thus fully recombining the viral cDNA with the host (reviewed in references 16 and 38).

IN functions as a multidomain protein consisting of the N-terminal domain (NTD), catalytic core domain (CCD), and C-terminal domain (CTD) as defined by limited proteolysis (29), deletion mutagenesis (9, 78), in vitro complementation assays (28, 77), and structural biology (14, 23, 79). The NTD (residues 1 to 49) harbors a conserved HHCC zinc binding motif that contributes to IN multimerization and catalytic function (8, 10, 24, 52, 86). The CCD (residues 50 to 212) contains an invariant triad of acidic residues (Asp-64, Asp-116, and Glu-152 of HIV-1) that form the D,D-35-E active-site motif (21, 29, 49, 51, 76). The CCD has an RNase H-fold, and the catalytic domains of certain bacterial transposases share this fold and also utilize invariant Asp and Glu residues for catalysis (see reference 71 for a review). Various assays have also defined residues within the CCD important for binding to viral and host DNA (20, 32, 36, 37, 41, 44).

Due to the relatively weak degree of sequence homology among retrovirus IN CTDs (a single invariant Trp at HIV-1 position 235), less is known about the precise roles of the CTD (residues 213 to 288) compared to the N-terminal and catalytic core domains in integration and HIV-1 replication. Results of several in vitro assays implicated retrovirus CTDs in DNA binding (31, 62, 78, 81, 82) and multimerization (1, 25, 43, 56). Residues 220 to 270 of HIV-1 IN define a minimal nonspecific DNA binding region (69), and Leu-234 (Val-234 in HIV-1 strain NL4-3, studied here), Arg-262, and Lys-264 contributed to this activity (68, 69). Since DNA protected Glu-246, Lys-258, and Lys-273 from proteolysis in vitro, these residues were also implicated in DNA binding (20) (Fig. 1A). The HIV-1 CTD also binds the viral *att* site: through Cys substitution, Glu-246 was found to cross-link to the adenine located 7 nucleotides from the end of the U5 plus strand (35). A limited number of viral mutants with changes at these amino acid positions, including HIV-$1_{K244A/E246A}$ (80), HIV-$1_{R262A/K264T}$ (11), and HIV-$1_{R262A/R263A/K264H}$ (64), have been analyzed. Although each virus was replication defective, contributions of individual residues to HIV-1 replication were unknown, since

* Corresponding author. Mailing address: Department of Cancer Immunology and AIDS, Dana-Farber Cancer Institute, 44 Binney Street, Boston, MA 02115. Phone: (617) 632-4361. Fax: (617) 632-3113. E-mail: alan_engelman@dfci.harvard.edu.

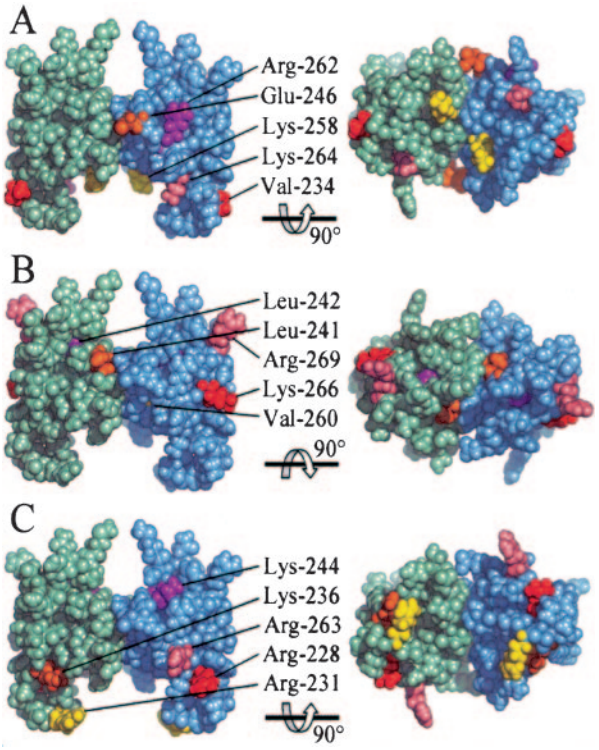

FIG. 1. CTD residues targeted in this study. (A) Residues implicated in binding to DNA. Amino acid side chains were highlighted on the dimeric NMR structure (Protein Data Bank entry 1IHV) (56) using the following coloring scheme: Val-234, red; Glu-246, orange; Lys-258, yellow; Arg-262, magenta; Lys-264, pink. The image to the right was rotated 90° along the horizontal axis, revealing the bottom of the structure on the left. Lys-273, also implicated in DNA binding (Table 1), is not shown, because it was not part of the structure. (B) Putative multimerization residues. Side chains were colorized as follows: Leu-241, orange; Leu-242, magenta; Val-260, yellow; Lys-266, red; Arg-269, pink. The image to the right was rotated 90° around the horizontal axis to reveal the top of the structure on the left. (C) Residues targeted due to relatively high degrees of sequence conservation. Arg-228, red; Arg-231, yellow; Lys-236, orange; Arg-263, pink; Lys-244, magenta. The image to the right was rotated as in panel A. The images were generated using PyMOL (17).

each mutant carried multiple amino acid substitutions and only a subset of potential DNA binding residues was targeted.

Results of a yeast two-hybrid assay identified Val-260 as important for IN multimerization (45), and 3-dimensional nuclear magnetic resonance (NMR) structures revealed Leu-241 and Leu-242 at or near a CTD dimer interface (25, 56) (Fig. 1B). Whereas HIV-1_{V260E} was replication defective (45), the roles of Leu-241 and Leu-242 in HIV-1 replication have not been investigated. A two-domain CCD-CTD variant solved by X-ray crystallography was also dimeric; however, dimerization was mediated via the CCDs, and the tethered CTDs were separated from each other by 55 Å (14). Nonetheless, novel CTD-CTD interactions were observed between crystallographic dimers, revealing potential roles for Lys-266 and/or Arg-269 in multimerization (14). Whereas a virus mutant altered at Lys-266 has not been described, HIV-$1_{R269A/D270A}$ transduced cells at approximately 15% of the wild-type (WT) level (80).

Replication-defective HIV-1 IN mutant viruses can be grouped into distinct phenotypic classes, for example, those specifically blocked at integration (class I IN mutants) versus those that display additional reverse transcription and/or particle assembly defects (class II mutants). Typified by changes in the D,D-35-E active-site residues, class I mutants support near-normal levels of reverse transcription, and because of this, transient increases in unintegrated viral DNA are observed during acute infection (26). Because the CTD mutant HIV-1_{W235E} was released normally from cells and supported the formation of more 2–long-terminal-repeat (2-LTR) circles than the WT (50), HIV-1_{W235E} was categorized as a class I mutant virus (26). Because HIV-1_{V260E} was released from transfected cells three to fivefold less efficiently than the WT (45), this replication-defective CTD mutant virus is defined here as class II.

In this study 16 CTD residues were targeted by mutagenesis, generating 24 mutant viruses. In addition to their potential roles in multimerization and DNA binding, residues were targeted due to their degree of sequence conservation among a large collection of HIV-1/SIV_{cpz} strains. The majority of replication-defective viruses displayed DNA synthesis and/or virus release defects, characterizing them as class II mutants. Of note, one novel mutant, HIV-1_{E246K}, supported near-WT levels of DNA synthesis and increased levels of 2-LTR circles despite an approximately 20-fold reduction in particle assembly and release. Unexpectedly, the E246K change inhibited proteolytic processing of $Pr55^{gag}$ in virus producer cells. HIV-1_{E246K} displayed about 8% of WT activity in a single-round infection assay, suggesting that perturbations of viral late events contributed significantly to the replication-defective phenotype. Results of Vpr-IN complementation assays revealed that the INs derived from most replication-defective CTD mutant viruses efficiently *trans*-complemented active-site mutant virus. Thus, despite replication-defective phenotypes, many CTD mutant IN proteins were catalytically active in the backdrop of HIV-1 infection.

MATERIALS AND METHODS

Plasmids. Viral mutations were introduced into pUCWTpol (53) using QuikChange mutagenesis (Stratagene, La Jolla, Calif.), and mutated 1.8-kb AgeI-PflMI *pol* fragments were swapped for the corresponding fragments in pNL43/XmaI (6) and envelope (Env)-deleted pNLX.Luc(R-) (57) to generate full-length proviral clones and single-round luciferase expression vectors, respectively. Plasmids encoding HIV-$1_{1–212}$, HIV-$1_{D64N/D116N}$ (63), HIV-$1_{V165A.Luc(R-)}$, and HIV-$1_{D64N/D116N.Luc(R-)}$ (57) have been described previously.

Expression vectors for vesicular stomatitis virus G (VSV-G) glycoprotein and HIV-1 NL4-3 Env (pNLXE7) have been described previously (53). Mutations were introduced into pRL2P-Vpr-IN (84) by QuikChange mutagenesis. Constructs encoding $Vpr\text{-}IN_{WT}$, $Vpr\text{-}IN_{V165A}$, $Vpr\text{-}IN_{Q62K}$, and $Vpr\text{-}IN_{D116A}$ have been described previously (57). Plasmid regions constructed by PCR were analyzed by DNA sequencing to confirm the desired mutations and the absence of off-site secondary changes.

Cells. 293T and HeLa cells were grown in Dulbecco's modified Eagle medium supplemented with 10% fetal calf serum, 100 IU/ml of penicillin, and 100 μg/ml of streptomycin. Jurkat T cells were grown in RPMI 1640 containing 10% fetal calf serum, 100 IU/ml of penicillin, and 100 μg/ml of streptomycin (RPMI). Monocyte-derived macrophages (MDM) were isolated from HIV-1-seronegative donors by plastic absorbance as previously described (63).

Viruses and infections. Transient transfection of 293T or HeLa cells by calcium phosphate generated viral stocks. Cell-free stocks were titered using an exogenous ^{32}P-based RT assay (30, 63) or the Alliance p24 ELISA kit (Perkin-Elmer Life Sciences, Boston, Mass.). Replication assays were performed by infecting 2×10^6 Jurkat T cells with 10^6 RT cpm of virus (approximate multiplicity of infection, 0.04 [54, 63]) for 17 h at 37°C. Infected cells were washed

TABLE 1. Targeted residues and mutant viruses

Residue	Conservation (% identity)[a]	Criterion for targeting[b]	Enzyme (% activity)[c]	Reference(s)	Mutant(s) analyzed
Arg-228	99.7	iii	R228I (10–50)[d]	69, 76	R228A
Arg-231	98.6	iii	R231A (10–50)	68	R231A
Val-234	12.5	i	L234A (50–100)	68	V234A
Lys-236	100	iii	K236S (>50)[d]	76, 80	K236A
					K236E
					K236A/E246A
Leu-241	99.7	ii, iii	L241A (0–10)	14, 25, 56, 68	L241A
Leu-242	99.7	ii, iii	L242A (0–10)	14, 25, 56, 68	L242A
Lys-244	99.7	iii	K244S (50–100)[d]	69, 76, 80	K244A
Glu-246	99.7	i, iii	E246A (50–100)	20, 35, 68, 80	E246A
			E246C (<100)		E246K
Lys-258	99.7	i, iii	K258L (50–100)[d]	20, 75, 76	K258A
			K258A (50–150)[d]		
Val-260	98.0	ii, iii	V260E (10–30)	45, 68	V260E
Arg-262	100	i, iii	R262D (10–50)[d]	35, 68, 69, 76	R262A
			R262G (53)		R262A/R263A
			R262C (<100)		R262A/K264A
					R262D/R263V/K264E (RRK/DVE)
Arg-263	99.7	iii	R263S (50–100)[d]	68, 69, 76	R263A
			R263V (>50)[d]		
			R263L (50–100)		
Lys-264	99.4	i, iii	K264E (1–10)[d]	69	K264A
					K264E
Lys-266	100	ii, iii		14	K266A
					K266E
Arg-269	76.5	ii	R269I (50–100)[d]	14, 76, 80	R269A
Lys-273	100	i, iii		20	K273A

[a] Relative to a collection of 345 HIV-1 and SIV_{cpz} strains (http://www.hiv.lanl.gov).
[b] i, putative role in DNA binding; ii, putative role in IN multimerization; iii, >95% identity as explained in footnote a.
[c] 3′ processing and/or DNA strand transfer activity.
[d] IN derived from HIV-2.

twice with serum-free RPMI, cultured in 5 ml of RPMI, and split at regular intervals, at which times supernatants were saved for RT assays.

Infections for real-time quantitative PCR (RQ-PCR) assays were performed as previously described (53, 57). Briefly, virus stocks generated by cotransfecting 293T cells with Env-deleted viral vectors and an Env expression plasmid were filtered and digested with 40 U/ml TURBO DNase (Ambion, Austin, Tex.) for 1 h at 37°C to remove residual plasmid DNA. Whereas 10^6 Jurkat cells were infected with 10^6 RT cpm of NL4-3-enveloped viruses by spinoculation, 4×10^6 cells were infected with 4×10^6 RT cpm of VSV-G pseudotypes. MDM were infected with 2×10^6 RT cpm of VSV-G pseudotypes for 2 h at 37°C without spinoculation.

RQ-PCR and single-round infectivity assays. DNAs from infected Jurkat cells and MDM were extracted using the DNeasy tissue kit as recommended by the manufacturer (QIAGEN, Valencia, Calif.). In duplicate 30-μl reaction mixtures, 10 μl of total DNA was analyzed for viral late reverse transcription (LRT) products and 2-LTR circles as previously described (53, 59). Values were normalized to those of cellular endogenous retrovirus-3 (ERV-3) as described elsewhere (53, 59). Parallel infections were performed with Env^- particles to assess residual levels of plasmid DNA that may have resisted DNase treatment, and these values were subtracted from results obtained with Env^+ viruses.

Jurkat cells harvested at 48 h postinfection (hpi) were washed with 1× phosphate-buffered saline (Mediatech, Herndon, Va.) and lysed in 75 μl of 1× passive lysis buffer (Promega Corp., Madison, Wis.). Frozen and thawed lysates were clarified by centrifugation at 18,730 × *g* for 15 min at 4°C, and supernatants (20 μl) were analyzed for luciferase activity in duplicate using the Promega luciferase assay system, an EG&G Berthold Microplate LB 96V luminometer, and a Microlite 1 flat-bottom microtiter plate (Thermo Labsystems, Franklin, Mass.). Luciferase activity was normalized to the protein concentration as determined by the Bio-Rad (Hercules, Calif.) assay and corrected for background levels from lysates of cells infected with Env^- controls.

Vpr-IN complementation assays. Viral stocks were generated by transfecting 293T cells with 2 μg of pNLX.Luc(R-), 1 μg of pRL2P-Vpr-IN, and 0.067 μg of pNLXE7. IN mutant infectivity in the absence of Vpr-IN was determined by replacing pRL2P-Vpr-IN with pcDNA3 (Invitrogen, Carlsbad, Calif.) during transfection. Jurkat cells (2×10^6) were infected with 5×10^5 RT cpm in 1 ml for 17 h at 37°C; then cultures were expanded to 5 ml using RPMI. Cell lysates prepared at 48 hpi were analyzed for luciferase activity as described above.

Radiolabeling and immunoprecipitation. HeLa cells (1.89×10^6) were transfected using calcium phosphate or FuGENE 6 with 20 or 10 μg of proviral DNA, respectively. Cells were metabolically labeled with [^{35}S]Cys and [^{35}S]Met (50 μCi/ml of each) from 48 to 60 h posttransfection. Saquinavir (10 μM final concentration) was added to transfected cells where indicated 8 h before radiolabeling. Labeled cells were lysed in a buffer containing 0.3 M NaCl, 50 mM Tris, pH 7.5, 0.5% Triton X-100 with 0.2 mM 4-(2-aminoethyl)benzenesulfonyl fluoride (AEBSF) and 100 μg/ml leupeptin (Roche Molecular Biochemicals, Indianapolis, Ind.). Cell lysates (1 ml) were spiked with 80 μl of 1% bovine serum albumin and precleared with 50 μl protein A-Sepharose CL-4B beads (Amersham Pharmacia Biotech AB, Uppsala, Sweden) hydrated in phosphate-buffered saline. Viral proteins were immunoprecipitated using AIDS patients' sera and separated by sodium dodecyl sulfate-polyacrylamide gel electrophoresis (SDS-PAGE). Virus particles were pelleted from cell supernatants by centrifugation (90 min at 4°C and 27,000 rpm in a Beckman SW28 rotor) through 20% sucrose cushions. Pelleted virions were lysed using 1× radioimmunoprecipitation assay buffer (140 mM NaCl, 8 mM Na_2HPO_4, 2 mM NaH_2PO_4, 1% Nonidet P-40, 0.5% sodium deoxycholate, 0.05% SDS), and particle-associated proteins were detected by SDS-PAGE and fluorography. Levels of p24 and $Pr55^{gag}$ in cellular and viral lysates were quantified by PhosphorImager analysis using ImageQuant, version 1.11 (Molecular Dynamics, Sunnyvale, Calif.).

RESULTS

Mutagenesis strategy. A total of 16 residues in the CTD of HIV-1 IN were targeted by mutagenesis, generating 24 mutant viruses (Table 1). Whereas Val-234, Glu-246, Lys-258, Arg-262, Lys-264, and Lys-273 (Fig. 1A) have been implicated in DNA binding (20, 35, 68, 69), Leu-241, Leu-242, Val-260, Lys-266, and Arg-269 (Fig. 1B) have been implicated in IN multimerization (14, 25, 45, 56, 68). The remaining five resi-

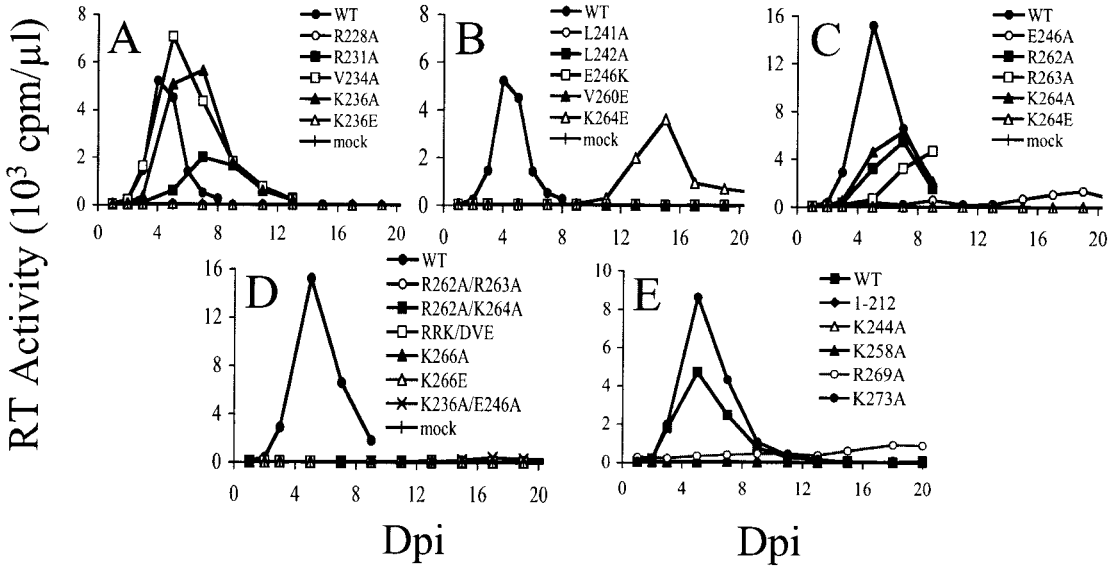

FIG. 2. WT and CTD mutant viral replication kinetics. Supernatants of cells infected with the indicated viruses were analyzed for RT activity at the indicated times. With the exception of HIV-1_{K264E}, independent experiments yielded similar results. HIV-1_{K264E} replicated 11 days after HIV-1_{NL4-3} in one experiment (B); however, the repeat experiment failed to reveal evidence of virus growth (C). We note that reversion of Glu back to Lys in HIV-1_{K264E} would require only one nucleotide change. Given the relatively robust growth observed at day 15 in panel B, we speculated that reversion to WT likely occurred in this experiment. Cultures that failed to support HIV-1 growth were monitored for 2 months. Dpi, days postinfection.

dues, Arg-228, Arg-231, Lys-236, Lys-244, and Arg-263 (Fig. 1C), were targeted due to their high degree of sequence conservation among HIV-1/SIV_{cpz} IN proteins (Table 1). Although single missense mutants of most of the residues were previously analyzed for 3′ processing and DNA strand transfer activities in in vitro integration assays (Table 1), only one mutant, HIV-1_{V260E} (45), was previously analyzed for the contribution of an individual residue to virus replication.

Replication profiles of CTD mutant viruses. Virus stocks generated by transient transfection were normalized for RT content, and target cells were challenged with equivalent RT cpm of WT or mutant virus. Jurkat cells infected at an approximate multiplicity of infection of 0.04 supported peak HIV-1_{NL4-3} replication 4 to 5 days postinfection (Fig. 2). As expected, the negative-control strain, HIV-$1_{1–212}$, which lacked the entire CTD (63), failed to replicate over 2 months of observation (Fig. 2E and data not shown). Also as expected (45), cells infected with HIV-1_{V260E} failed to yield a detectable level of virus growth (Fig. 2B). In contrast, approximately 30% of the mutant viruses replicated with near-WT kinetics (defined by the day at which peak replication was attained) (Table 2). These included HIV-1_{R231A}, HIV-1_{V234A}, HIV-1_{K236A} (Fig. 2A), HIV-1_{R262A}, HIV-1_{R263A}, HIV-1_{K264A} (Fig. 2C), and HIV-1_{K273A} (Fig. 2E). Although the single missense mutants HIV-1_{R262A}, HIV-1_{R263A}, and HIV-1_{K264A} replicated, multiple substitutions within this positively charged region yielded replication-defective mutants HIV-$1_{R262A/R263A}$, HIV-$1_{R262A/K264A}$, and HIV-$1_{RRK/DVE}$ (Fig. 2D). HIV-1_{R228A}, HIV-1_{K236E} (Fig. 2A), HIV-1_{L241A}, HIV-1_{L242A}, HIV-1_{E246K} (Fig. 2B), HIV-1_{K266A}, HIV-1_{K266E} (Fig. 2D), HIV-1_{K244A}, and HIV-1_{K258A} (Fig. 2E) were also dead viruses. Three mutants, HIV-1_{E246A} (Fig. 2C), HIV-$1_{K236A/E246A}$ (Fig. 2D), and HIV-1_{R269A} (Fig. 2E), exhibited significant although reproducible reductions in HIV-1 growth. Table 2 summarizes the phenotypes of the different mutant viruses.

DNA synthesis profiles of WT and IN mutant viruses. The preceding section revealed that a majority of CTD mutant viruses were blocked in their ability to replicate in Jurkat T cells, and the nature of the replication defects was investigated next. Replication-defective IN mutant viruses can be categorized into two distinct phenotypic groups (26). Class I IN mutants are specifically blocked at the integration step. Because reverse transcription proceeds normally, transient increases in unintegrated DNA such as 2-LTR circles are observed at a time when integration normally occurs (26). In contrast, class II mutants display pleiotropic defects that, in addition to integration, can affect late events such as particle assembly/release and/or the preintegration step of reverse transcription (26). Since class I IN mutant viruses yield increased levels of 2-LTR circles and class II mutants often display overall reductions in cDNA synthesis, RQ-PCR analysis of cDNA metabolism in acutely infected cells was utilized as an initial approach toward phenotypic classification. Taqman primers and probes were selected to detect products after the second template switch of reverse transcription as well as at the unique 2-LTR circle junction. Because reverse transcription peaks approximately 7 hpi and the peak of 2-LTR circles occurs about 24 hpi (12, 13, 46, 59), viral DNAs were analyzed at 7 and 24 hpi. To permit analyses in the absence of virus spread, mutations were introduced into the single-round, Env-deleted HIV-$1_{NLX.Luc(R-)}$ strain, which carried firefly luciferase in the viral *nef* position (57). Controls included the previously described CTD class I mutant HIV-$1_{W235E.Luc(R-)}$ (50) and the CCD class II mutant HIV-$1_{V165A.Luc(R-)}$ (53, 57).

HIV-$1_{W235E.Luc(R-)}$ supported near-WT levels of DNA synthesis (differing by twofold at most) at 7 and 24 hpi (Fig. 3A, C,

TABLE 2. HIV-1 IN CTD mutant phenotypes

Mutant	Replication[a]	DNA synthesis[b]	2-LTR[c]	Infectivity[d]	Phenotype[e]
R228A	−	−	ND	0.18 (0.25)	II
R231A	+	NA[f]	NA	NA	NA
V234A	+	NA	NA	NA	NA
K236A	+	NA	NA	NA	NA
K236E	−	+	+	0.07 (0.04)	II
K236A/E246A	+/−	+	++	4.0 (0.3)	II[g]
L241A	−	−	+	0.00 (0.00)	II
L242A	−	−	+	0.13 (0.19)	II
K244A	−	−	++	0.21 (0.13)	II
E246A	+/−	+	++	26.3 (3.2)	II[g]
E246K	−	++	++	8.4 (4.0)	II
K258A	−	−	+	0.09 (0.01)	II
V260E	−	−	−	0.00 (0.00)	II
R262A	+	NA	NA	NA	NA
R262A/R263A	−	+/−	+/−	0.01 (0.00)	II
R262A/K264A	−	+	+	0.01 (0.00)	II
RRK/DVE	−	+/−	+	0.02 (0.00)	II
R263A	+	NA	NA	NA	NA
K264A	+	NA	NA	NA	NA
K264E	−	+/−	++	0.11 (0.00)	II
K266A	−	+/−	−	0.00 (0.00)	II
K266E	−	−	+	0.00 (0.00)	II
R269A	+/−	+	++	11.5 (2.3)	I[g]
K273A	+	NA	NA	NA	NA

[a] As determined in Fig. 2. +, replication peak detected up to 4 days delayed relative to the WT; +/−, peak detected up to 12 days delayed relative to the WT concurrent with an 8- to 20-fold reduction in RT activity; −, replication not detected after 2 months of observation. Values represent results of duplicate infections.

[b] Late reverse transcription products at 7 h postinfection (Fig. 3). ++, >50% of WT; +, 20 to 50% of WT; +/−, 10 to 20% of WT; −, <10% of WT.

[c] 2-LTR circles at 24 h postinfection (Fig. 3). ++, >50% of WT; +, 20 to 50% of WT; +/−, 10 to 20% of WT; −, limit of detection to 10% of WT; ND, not detected (2-LTR circles below the limit of detection [<6.0% of WT]).

[d] Average values for duplicate luciferase assays and a minimum of two independent infections, with standard deviations given in parentheses.

[e] Based on results in Fig. 2 to 6. Whereas class I mutants are specifically blocked at integration, class II mutants display additional reverse transcription and/or release defects.

[f] NA, not applicable; the virus was classified as WT.

[g] Although the class I/II nomenclature usually applies to completely dead viruses, here it indicates whether the primary replication block (Fig. 2) was at integration (class I) or also encompassed reverse transcription and virus release (class II).

and E). As predicted for the class I mutant phenotype, HIV-$1_{W235E.Luc(R-)}$ yielded up to 12-fold more 2-LTR circles than the WT at 24 hpi (Fig. 3B, D, and F). In contrast, the class II control HIV-$1_{V165A.Luc(R-)}$ supported significantly less (approximately 10 to 20-fold) reverse transcription than the WT (Fig. 3A, C, and E), and as previously described (57), mutant 2-LTR circle levels mirrored these overall reductions in DNA synthesis (Fig. 3B, D, and F). In other words, the percentages of total viral cDNA converted to 2-LTR circles were similar for HIV-$1_{NLX.Luc(R-)}$ and HIV-$1_{V165A.Luc(R-)}$.

Replication-defective CTD mutants displayed a wide range of DNA synthesis profiles that varied from WT levels (for example, HIV-$1_{E246K.Luc(R-)}$ at 24 hpi [Fig. 3A]) to approximately 2% of WT (HIV-$1_{R228A.Luc(R-)}$ [Fig. 3A]). Mutants with >10-fold DNA synthesis defects at 7 hpi included HIV-$1_{R228A.Luc(R-)}$, HIV-$1_{L242A.Luc(R-)}$, HIV-$1_{K244A.Luc(R-)}$ (Fig. 3A), HIV-$1_{L241A.Luc(R-)}$, HIV-$1_{K258A.Luc(R-)}$, HIV-$1_{V260E.Luc(R-)}$ (Fig. 3C), and HIV-$1_{K266E.Luc(R-)}$ (Fig. 3E) (Table 2). Somewhat less severe 5- to 10-fold defects were detected for HIV-$1_{R262A/R263A.Luc(R-)}$, HIV-$1_{R262A/K264A.Luc(R-)}$, HIV-$1_{K264E.Luc(R-)}$ (Fig. 3C), and HIV-$1_{RRK/DVE.Luc(R-)}$ (Fig. 3E), and moderate 2- to 4-fold defects were detected for HIV-$1_{K236E.Luc(R-)}$, HIV-$1_{E246K.Luc(R-)}$ (Fig. 3A), HIV-$1_{K236A/E246A.Luc(R-)}$ (Fig. 3C), and HIV-$1_{R269A.Luc(R-)}$ (Fig. 3E). Although the twofold reduction for HIV-$1_{K266A.Luc(R-)}$ was similar to that of the class I HIV-$1_{W235E.Luc(R-)}$ control in Fig. 3E, we note that repeat experiments revealed an approximately 5- to 10-fold DNA synthesis defect for HIV-$1_{K266A.Luc(R-)}$ (Fig. 4A; data not shown; Table 2).

Since 2-LTR circles are thought to form in the nuclei of HIV-1-infected cells, their detection affords a convenient marker for the nuclear localization of nascent cDNA (reviewed in reference 38). For most of the mutants, the percentage of LRT cDNA converted to 2-LTR circles was greater than or similar to that for the WT. Two notable exceptions were HIV-$1_{K266A.Luc(R-)}$, which, based on total cDNA levels, yielded six- to eightfold-lower levels of 2-LTR circles than the WT (Fig. 3F and 4C), and HIV-$1_{R228A.Luc(R-)}$, where 2-LTR circles were initially undetectable (Fig. 3B). Because the lack of detection of HIV-$1_{R228A.Luc(R-)}$-derived circles was likely due to the low level of cDNA synthesis (Fig. 3A), the VSV-G Env glycoprotein was utilized to increase the efficiency of virus entry. Because nondividing cells such as MDM present a paradigm for active HIV-1 nuclear import (73), this cell type was analyzed alongside Jurkat T cells.

As expected, Jurkat cells infected with VSV-G-pseudotyped virus supported significantly more reverse transcription than cells infected via HIV-1 Env glycoproteins (compare Fig. 4B to 4A). In this experiment, the level of HIV-$1_{R228A.Luc(R-)}$ cDNA synthesis was reduced only about fourfold from the WT level, revealing a normal fraction of 2-LTR circles following HIV-1-Env-mediated entry (Fig. 4A and C). As previously observed (57), IN mutant viral DNA synthesis defects relative to WT DNA synthesis were maintained despite the overall increases in reverse transcription imparted via VSV-G (Fig. 4A and B). The class I mutant control strain HIV-$1_{D64N/D116N.Luc(R-)}$ (58) formed significantly more 2-LTR circles than WT HIV-$1_{NLX.Luc(R-)}$, independently of the route of viral entry (Fig. 4C and D). Levels of VSV-G-mediated HIV-$1_{K266A.Luc(R-)}$ and HIV-$1_{R228A.Luc(R-)}$ 2-LTR circles mirrored overall mutant cDNA levels in Jurkat cells, indicating efficient nuclear import of viral cDNA complexes under these conditions (compare Fig. 4C and D to 4A and B, respectively). VSV-G-pseudotyped HIV-$1_{K266A.Luc(R-)}$ and HIV-$1_{R228A.Luc(R-)}$ also converted near-normal fractions of their cDNAs to 2-LTR circles in MDM (Fig. 4E and F). We therefore concluded that the low levels of HIV-$1_{R228A.Luc(R-)}$ (Fig. 3B) and HIV-$1_{K266A.Luc(R-)}$ (Fig. 4C) DNA circles observed in some experiments were due primarily to the extremely low levels of reverse transcription that had occurred in these cases (Fig. 3A and 4A).

Mutant virus release from cells. In addition to reverse transcription, some class II mutants are defective for virus assembly and release (26). To assess release, levels of cell supernatant RT activity were quantified following transient transfection of $CD4^-$ HeLa cells. The CD4-negative phenotype permitted comparison of replication-defective and replication-competent strains. Previous analyses revealed that class

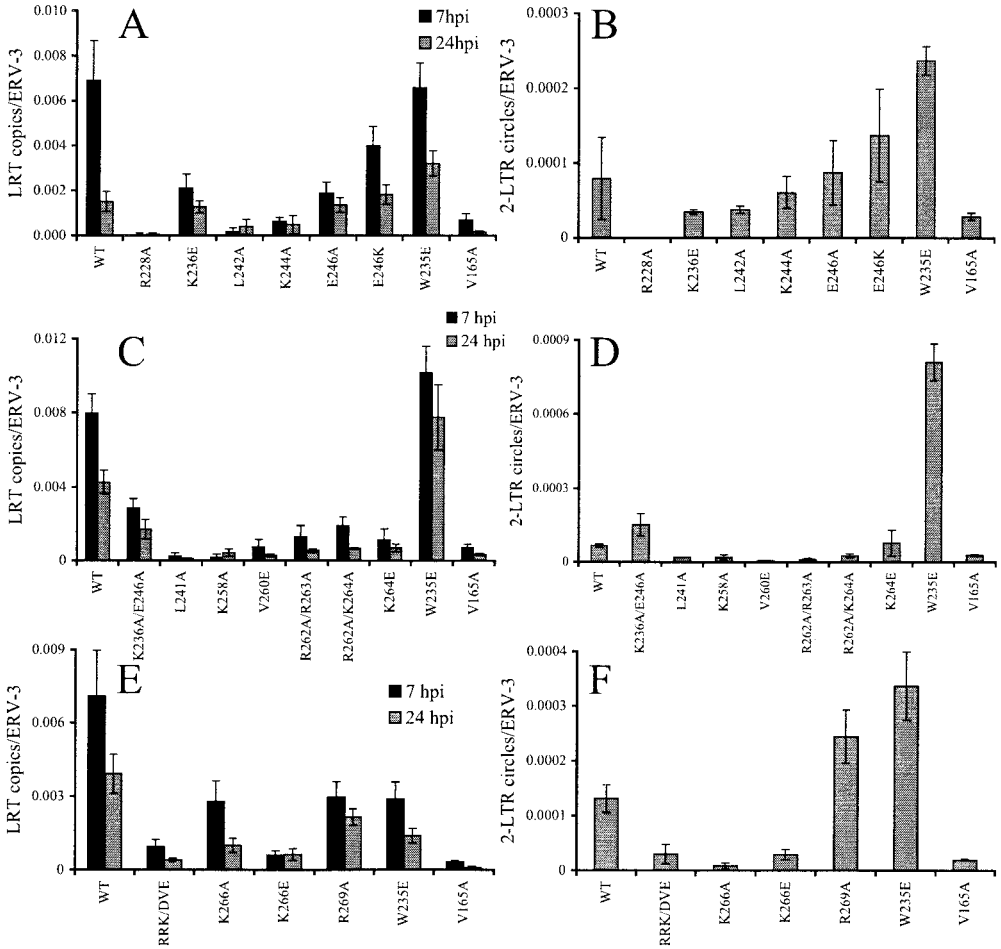

FIG. 3. Mutant viral cDNA metabolism. (A, C, and E) DNA was isolated at 7 (black bars) and 24 (gray bars) hpi from Jurkat cells infected with the indicated single-round viruses. HIV-1 levels were normalized to ERV-3 by RQ-PCR. (B, D, and F) 2-LTR circle levels at 24 hpi. Error bars represent variation between duplicate RQ-PCR assays. Similar results were obtained following an independent set of infections.

II mutant strains expressed HIV-1 proteins at WT levels (reference 57 and references therein).

The class I mutant control strain HIV-$1_{D64N/D116N}$ was released from HeLa cells at the WT level (Fig. 5A). In contrast, the CTD deletion mutant HIV-$1_{1–212}$ was about fourfold defective for release (Fig. 5A). Most of the replication-defective CTD mutants either were released at the WT level or showed marginal (approximately 1.5- to 3-fold) release defects. Two notable exceptions were HIV-$1_{RRK/DVE}$ and HIV-1_{E246K}: whereas HIV-$1_{RRK/DVE}$ behaved similarly to the HIV-$1_{1–212}$ control (approximate fourfold defect), HIV-1_{E246K} was released at only about 5% of the WT level (Fig. 5A). Because RT interacts with IN through the CTD (40, 87), CTD mutations could in theory alter RT packaging and/or virion-associated activity. To address this potential caveat, a subset of the mutant viruses was analyzed for p24 levels, and these values were compared to corresponding RT activities in HeLa cell supernatants. The results of this analysis revealed that p24 and RT levels closely mirrored each other in the majority of cases, although the RT activity of HIV-$1_{RRK/DVE}$ was approximately twofold lower than the corresponding p24 value (Fig. 5B). These results are in line with previous observations that mutations only minimally altered the p24-to-RT ratio of CTD mutant viruses (11).

Based on WT and mutant cDNA synthesis (Fig. 3 and 4) and virus release (Fig. 5) profiles, we concluded that the majority of the replication-defective CTD mutants were phenotypically class II (Table 2). Since HIV-1_{R269A} was released at the WT level (Fig. 5), supported near-WT levels of DNA synthesis, and converted more of its cDNA to LTR circles than the WT (Fig. 3), it was typed as a class I mutant (Table 2).

Processing defect of HIV-1_{E246K}. The release defect associated with IN deletion mutant viruses can be overcome by inhibiting the activity of the viral protease through mutation or treatment with antiviral compounds (7). To further probe the dramatic reduction in HIV-1_{E246K} release, transfected HeLa cells metabolically labeled with [^{35}S]Met and [^{35}S]Cys were either left untreated or treated with the protease inhibitor saquinavir, and cell- and virion-associated HIV-1 proteins were visualized following SDS-PAGE and fluorography. To aid detection of cell-associated proteins, lysates were immunoprecipitated with AIDS patients' sera prior to electrophoresis. In contrast, virion proteins were recovered following direct pelleting of cell supernatants through sucrose cushions.

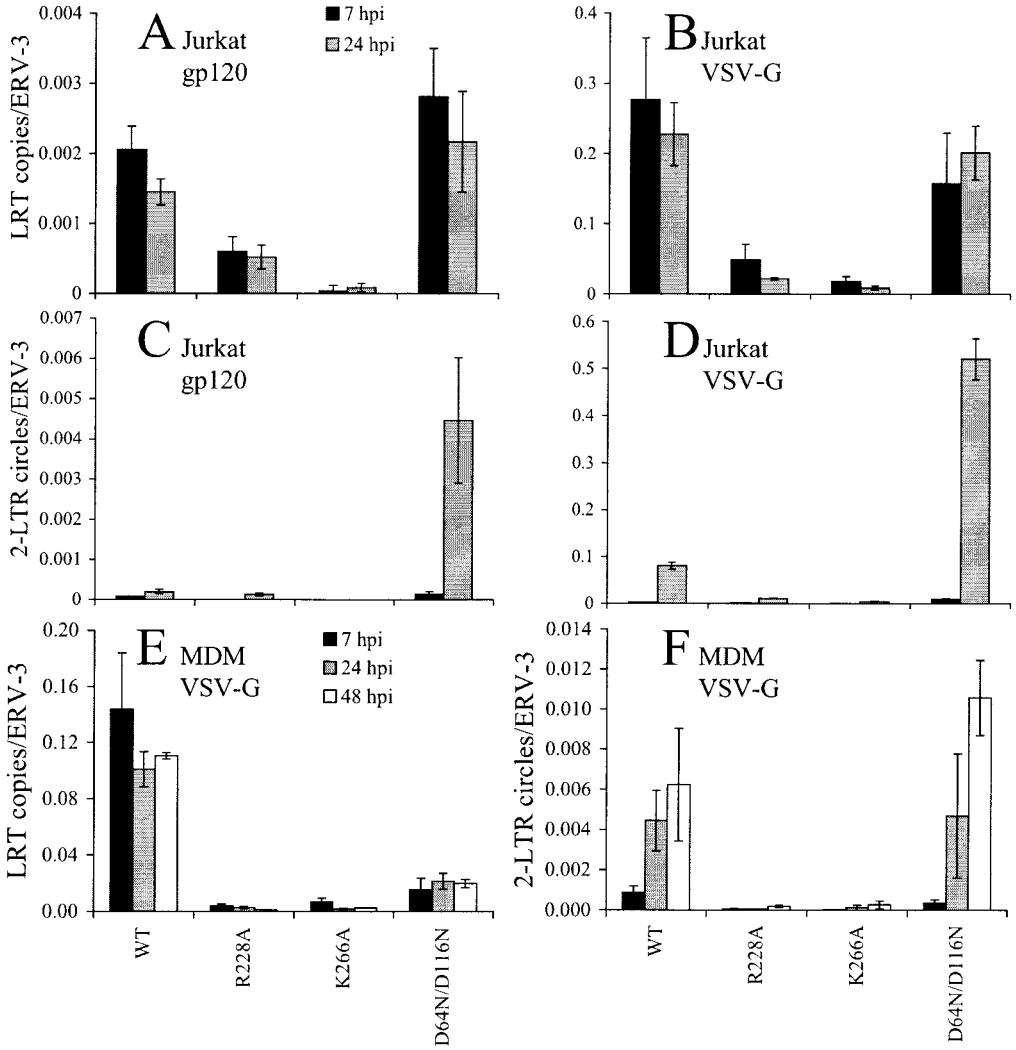

FIG. 4. HIV-$1_{K266A.Luc(R-)}$ and HIV-$1_{R228A.Luc(R-)}$ DNA levels following VSV-G-mediated entry. (A) DNA was isolated at 7 (black bars) and 24 (gray bars) hpi from Jurkat cells infected with the indicated single-round viruses carrying the HIV-1 Env glycoprotein. HIV-1 LRT levels were normalized to ERV-3 following RQ-PCR. (B) Same as panel A except that viruses were pseudotyped with VSV-G. (C and D) Normalized levels of 2-LTR circles in extracts from panels A and B, respectively. (E) DNA was isolated at 7 (black bars), 24 (gray bars), and 48 (white bars) hpi from MDM infected with the indicated VSV-G-pseudotypes. LRT levels were normalized to ERV-3. (F) Normalized levels of 2-LTR circles in MDM extracts. Error bars, variation obtained between duplicate RQ-PCR assays. Similar results were obtained following independent sets of Jurkat cell and MDM infections.

Processed p24 and precursor $Pr55^{gag}$ proteins were identified in WT HIV-1_{NL4-3}-expressing cells (Fig. 6A, lane 3). Saquinavir effectively inhibited WT polyprotein processing: the level of cellular $Pr55^{gag}$ increased at the expense of p24 production (Fig. 6A, lane 4), and $Pr55^{gag}$ instead of p24 was released from cells (Fig. 6B, compare lane 4 to lane 3). As previously observed for IN deletion mutants (7, 58, 70), intracellular $p41^{gag}$ and p25 processing intermediates were detected in HIV-$1_{1–212}$-expressing cells (Fig. 6A, lane 5), and in agreement with Fig. 5A, extracellular HIV-$1_{1–212}$ p24 levels were reduced about fourfold from the WT level (Fig. 6B, compare lane 5 to lane 3). Also as previously established (7), saquinavir effectively counteracted the HIV-$1_{1–212}$ release defect: substantial levels of pelletable $Pr55^{gag}$ were recovered after drug treatment (Fig. 6B, lane 6). In contrast to both the WT and the HIV-$1_{1–212}$ deletion mutant, HIV-1_{E246K} was poorly processed in cells; only a minimal level of p24 was detected (Fig. 6A, lane 7). Whereas saquinavir effectively blocked HIV-1_{E246K} processing (Fig. 6A, lane 8), it did not enhance the release of polyprotein precursors (Fig. 6B, lanes 7 and 8). Based on this, we concluded that the E246K mutation impacted HIV-1 late events differently than previously characterized class II IN deletion mutations.

Single-round infectivities of CTD mutant viruses. The experiment for which results are shown in Fig. 2 measured infectivity as a function of virus spread. Since some CTD mutants were released from cells less efficiently than the WT (Fig. 5 and 6), it was of interest to also determine infectivity in the absence of virus spread. In other words, by quantifying luciferase activity in cell extracts following single-round infections, infectivity would be determined independently of potential viral late event (release/processing) defects. A subset of the cells that

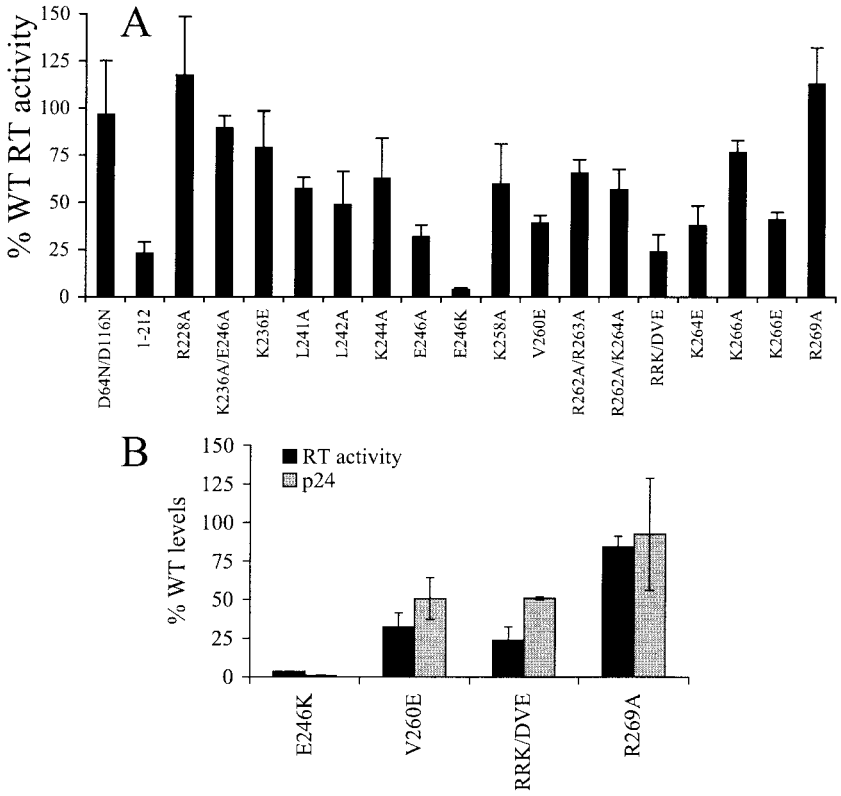

FIG. 5. Virus release from HeLa cells. (A) Results of duplicate RT assays following a minimum of three independent transfections, expressed as percentages of WT activity. (B) Results of duplicate RT and p24 assays following two independent transfections, expressed as percentages of WT values.

were infected for RQ-PCR measurements was lysed at 48 hpi, and luciferase activity was normalized to total cell protein concentration.

Whereas the infectivity of the class I mutant control strain HIV-$1_{W235E.Luc(R-)}$ was 0.39% ± 0.23% that of the WT, the class II HIV-$1_{V165A.Luc(R-)}$ mutant supported 0.01% ± 0.02% of WT activity. Each replication-defective CTD mutant fell within this low to background range of luciferase activity with the exception of HIV-$1_{E246K.Luc(R-)}$, which displayed about 8% of the WT titer (Table 2). HIV-$1_{K236A/E246A}$, HIV-1_{E246A}, and HIV-1_{R269A}, each of which supported low but reproducible levels of virus spread (Fig. 1), also supported luciferase activities that were significantly above background (Table 2).

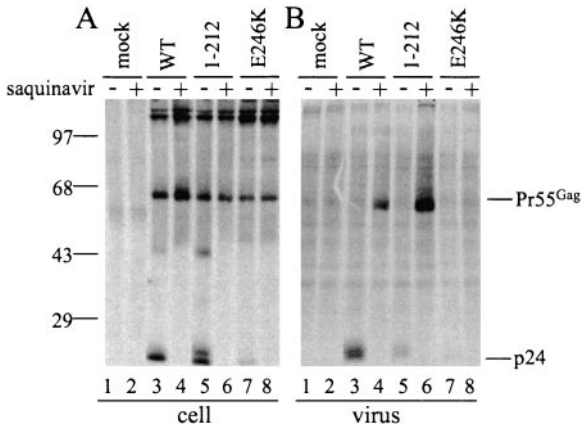

FIG. 6. Defective HIV-1_{E246K} processing. (A) Cell-associated proteins. Cells were treated with saquinavir as indicated prior to radiolabeling, and cell lysates were immunoprecipitated prior to SDS-PAGE. (B) Virion proteins. Cell supernatants pelleted through sucrose were lysed prior to electrophoresis. Migration positions of molecular mass standards are indicated on the left, and $Pr55^{gag}$ and p24 are indicated on the right. Similar results were observed in three independent experiments.

Vpr-IN complementation. Results of in vitro complementation assays established that IN comprised three distinct functional domains, the NTD, CCD, and CTD. Whereas two proteins containing mutations in different domains could functionally complement each other, proteins with mutations in the same domain failed to restore IN function (28, 77). Complementation-dependent rescue of IN function can also occur during HIV-1 infection. The infectivity defect of IN mutant viruses can be rescued by *trans*-incorporating IN_{WT} as a Vpr-IN fusion protein during HIV-1 assembly (33, 84). In addition, Vpr-IN proteins derived from certain replication-defective IN mutant viruses restored infectivity to class I active-site CCD mutant viruses (5, 33, 57, 58, 67). Notably, since a subset of these (class II) IN mutations also resided in the CCD, complementation in vivo can extend beyond the traditional definition of IN domain boundaries (57, 58). Class II CCD mutant INs efficiently *trans*-complemented class I CCD mutant viruses because the class II mutant proteins retained catalytic activity (57).

The results presented in Fig. 2 to 6 led to phenotypic classification of the majority of CTD mutant viruses as class II (Table 2). To investigate the catalytic potential of CTD mutant proteins as well as the interplay between the CCD and CTD during integration, a subset of mutations that addressed the multiple roles of the CTD, including R228A, L242A, E246K, K258A, V260E, K264E, and K266A (see Table 1), was introduced into a Vpr-IN expression vector. The following control changes were also studied: W235E (a CTD class I mutation), Q62K and D116A (CCD class I mutations [57]), and V165A (a CCD class II mutation [57]). Vpr-IN proteins were tested for their ability to *trans*-complement four different single-round mutant viruses: HIV-$1_{D64N/D116N.Luc(R-)}$ (an active-site CCD class I mutant), HIV-$1_{V165A.Luc(R-)}$ (a CCD class II mutant), HIV-$1_{W235E.Luc.(R-)}$ (CTD; class I), and HIV-$1_{1–212.Luc(R-)}$ (CTD; class II). Levels of Vpr-IN mutant complementation activity were quantified as percentages of Vpr-IN_{WT} activity (Table 3). We note that the baseline infectivity of 0.39% ± 0.23% reported for HIV-$1_{W235E.Luc(R-)}$ in the preceding section is greater than the Table 3 value of 0.02% ± 0.01% due to different multiplicities of infections that were utilized in the different experiments.

As expected (5), Vpr-IN_{V165A} efficiently complemented HIV-$1_{D64N/D116N.Luc(R-)}$ under conditions where it failed to complement HIV-$1_{V165A.Luc(R-)}$ (57) (Table 3). Conversely, neither Vpr-IN_{Q62K} nor Vpr-IN_{D116A} complemented HIV-$1_{D64N/D116N.Luc(R-)}$, but each partially restored HIV-$1_{V165A.Luc(R-)}$ infectivity (57) (Table 3). In contrast to the differential behavior of CCD class I versus class II Vpr-IN mutant proteins with class I and class II CCD mutant viruses, the CCD mutant proteins behaved similarly with class I (HIV-$1_{W235E.Luc(R-)}$) and class II (HIV-$1_{1–212.Luc(R-)}$) CTD mutant viruses. Whereas each functionally complemented HIV-$1_{W235E.Luc.(R-)}$, none functioned with HIV-$1_{1–212.Luc(R-)}$ (Table 3). The inability to complement HIV-$1_{1–212.Luc(R-)}$ was somewhat surprising, since each CCD mutant protein contained an intact CTD.

Vpr-IN_{W235E} rescued the infectivity of each virus tested, including HIV-$1_{W235E.Luc.(R-)}$ (Table 3). Complementation of defective IN mutant virus by Vpr-mediated *trans*-incorporation of the same mutant protein has been observed previously (57, 67) and likely depends on the inherent activity of the IN mutant protein (IN_{W235E} displayed WT function in an in vitro integration assay [51]) and the incorporation of greater than normal levels of IN protein during virus assembly (57, 58, 67). In contrast to Vpr-IN_{W235E}, the function of Vpr-IN_{V260E} was fairly inefficient; it yielded only about 5% of Vpr-IN_{WT} activity with HIV-$1_{D64N/D116N.Luc(R-)}$ and negligible levels of complementation with HIV-$1_{V165A.Luc(R-)}$, HIV-$1_{W235E.Luc.(R-)}$, and HIV-$1_{1–212.Luc(R-)}$ (Table 3). These results likely reflect the innate activity of the mutant enzyme, which was previously reported at approximately 10% of IN_{WT} activity in in vitro integration assays (68).

With the exception of Vpr-IN_{V260E}, each novel CTD mutant fusion protein efficiently complemented $HIV_{D64N/D116N.Luc(R-)}$ (~18% to 320% of Vpr-IN_{WT} activity [Table 3]). Because of this, we concluded that each of these IN enzymes could support substantial levels of integration during infection and, by extension, that each Vpr-IN protein was efficiently incorporated into particles during cotransfection. Since Vpr-IN_{R228A},

TABLE 3. Complementation of IN mutant viruses with Vpr-IN[a]

IN mutant	% of WT luciferase activity[b] (SD)		Luciferase activity after complementation with the following Vpr-IN mutant relative to activity after complementation with Vpr-IN_{WT}[c]:									
	Without complementation	After complementation with Vpr-IN_{WT}	R228A	L242A	E246K	K258A	V260E	K264E	K266A	W235E	V165A	Q62K	D116A
V165A	0.00 (0.00)	14.6 (1.3)	3.7 (0.0)	−0.1 (0.0)	13.3 (0.4)	10.4 (1.2)	0.0 (0.1)	27.9 (7.5)	−0.2 (0.0)	58.7 (11.1)	0.0 (0.2)	26.0 (10.6)	7.6 (5.1)
D64N/D116N	0.06 (0.03)	11.0 (0.4)	100.6 (10.1)	45.8 (8.0)	17.7 (2.1)	320.9 (86.7)	5.0 (0.1)	68.1 (10.1)	31.6 (8.6)	93.9 (0.1)	67.6 (1.7)	0.2 (0.1)	0.0 (0.1)
1-212	0.00 (0.01)	9.8 (1.7)	4.0 (1.9)	0.3 (0.2)	4.4 (0.3)	5.2 (2.9)	0.4 (.1)	1.8 (0.7)	0.3 (0.3)	28.6 (4.7)	0.9 (0.9)	1.8 (2.2)	3.0 (3.7)
W235E	0.02 (0.01)	27.2 (2.5)	20.5 (3.9)	15.7 (2.2)	9.1 (1.2)	183.4 (16.2)	1.1 (0.7)	5.3 (0.1)	2.7 (0.8)	11.9 (4.0)	36.0 (2.2)	35.4 (4.7)	11.8 (2.0)

[a] Values represent an average of at least two infections.
[b] Luciferase activity of the indicated IN mutant virus relative to that of HIV-$I_{Luc(R-)}$.
[c] Expressed as a percentage (with the standard deviation in parentheses).

Vpr-IN$_{L242A}$, and Vpr-IN$_{K266A}$ failed to appreciably complement HIV-1$_{V165A.Luc(R-)}$, we concluded that R228A, L242A, V260E, and K266A belonged to the same complementation group as V165A (Table 3). Apart from Vpr-IN$_{WT}$ and Vpr-IN$_{W235E}$, none of the Vpr-IN fusions appreciably complemented HIV-1$_{1–212.Luc(R-)}$, although Vpr-IN$_{R228A}$, Vpr-IN$_{E246K}$, and Vpr-IN$_{K258A}$ did support approximately 4% to 5% of Vpr-IN$_{WT}$ activity (Table 3). Each of these novel proteins efficiently complemented HIV-1$_{W235E.Luc(R-)}$ (~9% to 180% of Vpr-IN$_{WT}$), as did Vpr-IN$_{L242A}$ (Table 3).

DISCUSSION

Previous analyses of in vitro integration activities suggested that the CTD of HIV-1 IN was essential for enzymatic function (28, 78). Consistent with these observations, HIV-1$_{1–212}$, lacking the entire CTD (63), and a number of CTD missense mutant viruses were defective in assays for HIV-1 infectivity (11, 45, 50, 64, 80).

CTD DNA binding activity and HIV-1 replication. Soon after reverse transcription, a multimer of IN site-specifically recognizes the viral *att* sites and hydrolyzes a dinucleotide from each 3′ end. In addition to site-specific *att* site binding, the IN multimer must nonspecifically interact with chromosomal DNA during strand transfer. The original function ascribed to the HIV-1 IN CTD was that of nonspecific DNA binding, leading to suggestions that the domain might represent the major determinant of chromosomal DNA recognition during integration (31, 78, 82). A variety of residues, including Val-234, Glu-246, Lys-258, Arg-262, Lys-264, and Lys-273, were implicated in nonspecific DNA binding activity (20, 68, 69). More recently, it has become clear that the IN CCD contains important nonspecific DNA binding determinants (3, 39, 72) and that Glu-246 within the CTD can interact with the viral *att* site during integration (35). Whereas HIV-1$_{K244A/E246A}$ (80), HIV-1$_{R262A/K264T}$ (11), and HIV-1$_{R262A/R263A/K264H}$ (64) were noninfectious, the contribution of individual DNA binding residues to HIV-1 replication was unknown. Since HIV-1$_{V234A}$ (Fig. 2A) and HIV-1$_{K273A}$ (Fig. 2E) grew like WT HIV-1 $_{NL4-3}$, our results failed to support an important role for either Val-234 or Lys-273 in HIV-1 replication. Although the majority of HIV-1/SIV$_{cpz}$ strains harbor Ile, Ser and His are occasionally found at position 234 (47). In this light, it was not overly surprising that HIV-1$_{V234A}$ replicated like the WT. Since Lys-273 is invariant among HIV-1 and related chimpanzee strains (47), a potential role for this residue in HIV-1 replication could lie outside the realm of spreading infection in Jurkat T cells.

HIV-1$_{R262A}$, HIV-1$_{R263A}$, and HIV-1$_{K264A}$ grew similarly to the WT, yet HIV-1$_{K264E}$, HIV-1$_{R262A/R263A}$, and HIV-1$_{R262A/K264A}$ were replication defective (Fig. 2 and Table 2). This suggests that the HIV-1$_{K264E}$ replication defect was due primarily to the negative impact of the nonconservative Glu substitution rather than to a necessity for Lys at this position. Since HIV-1$_{K264E}$, HIV-1$_{R262A/R263A}$, and HIV-1$_{R262A/K264A}$ were 5- to 10-fold defective for cDNA synthesis and 1.4- to 3-fold reduced for viral release, they were typed as class II IN mutant viruses (Fig. 3 and 5; Table 2).

We recently determined via Vpr-IN complementation assays that certain CCD class I and class II mutants functioned as separate complementation groups, which revealed that this type of classI/II complementation can extend beyond the traditional boundaries of IN domain structure (57). Because the class II CCD mutant proteins retained catalytic function, we and others proposed that the mutations were likely to affect higher-order interactions between IN and other proteins specific to the infected cell such as RT and/or host cell factors (22, 57). By extending these analyses to include a variety of CTD mutant proteins and viruses, we determined additional examples of class I/II complementation as well as examples of traditional domain boundary complementation. Because Vpr-IN$_{K264E}$ efficiently complemented HIV-1$_{D64N/D116N.Luc(R-)}$ and HIV-1$_{V165A.Luc(R-)}$ under conditions where HIV-1$_{1–212.Luc(R-)}$ and HIV-1$_{W235E.Luc(R-)}$ complementation was more marginal (Table 3), we conclude that the Lys-to-Glu change disrupted a CTD function that was readily complemented by CCD mutant viruses regardless of their class I or class II phenotype. Since IN$_{K264E}$ was defective for DNA binding (69), we speculate that this CTD function can be provided in *trans* by different classes of CCD mutant viruses during HIV-1 infection. Because of this, we concluded that class I and class II need not always define separate complementation groups in vivo. On the other hand, Vpr-IN$_{K258A}$ functioned for the most part in a manner blind to IN domain boundaries: complementation of class II HIV-1$_{V165A.Luc(R-)}$ and HIV-1$_{1–212.Luc(R-)}$ mutant viruses occurred at only about 2% to 6% of the level of class I mutant virus rescue (Table 3). Although Lys-258 was also implicated in DNA binding (20), our results suggest that the K258A mutation affected a function(s) that is similarly perturbed by other class II mutations and thus might affect protein-protein interactions (57) in addition to potential IN-DNA interactions.

CTD multimerization and HIV-1 replication. Previous in vitro work highlighted the importance of CTD-dependent multimerization in IN function (1, 43), and the virus-based results reported here support this contention. Viruses mutated at previously implicated multimerization determinants were either dead (HIV-1$_{L241A}$, HIV-1$_{L242A}$, HIV-1$_{V260E}$, HIV-1$_{K266A}$, HIV-1$_{K266E}$) or severely impaired (HIV-1$_{R269A}$) in their ability to replicate (Table 1 and Fig. 2). Since HIV-1$_{K266A}$ and HIV-1$_{K266E}$ were both replication defective, our results indicate that it is particularly important for HIV-1 to harbor a positively charged side chain at this position. Since Lys-266 is solvent accessible and diametrically opposed to the dimer interface in the NMR structure of the CTD (Fig. 1B), the crystallographic CTD-CTD contact mediated via Lys-266 (14) may be of importance during HIV-1 infection. HIV-1$_{K266A}$ and HIV-1$_{K266E}$, as well as HIV-1$_{L241A}$, HIV-1$_{L242A}$, and HIV-1$_{V260E}$, were typed as class II mutant viruses (Fig. 3 to 5; Table 2). Like Val-260, Leu-242 is for the most part buried within the core of the CTD structure (Fig. 1B). Because of this, it was not overly surprising that HIV-1$_{L242A}$ displayed pleiotropic replication defects.

Vpr-IN$_{L242A}$ complemented class I mutant viral strains under conditions where class II mutant complementation was not observed (Table 3). Thus, Vpr-IN$_{L242A}$ functioned as a class II mutant compared to a traditional CTD mutant under these assay conditions. The function of Vpr-IN$_{K266A}$ was somewhat less clear, although due to the strikingly different results obtained with HIV-1$_{D64N/D116N.Luc(R-)}$ versus HIV-1$_{V165A.Luc(R-)}$, it too seemed to demonstrate mainly class II behavior during

complementation (Table 3). The finding that changes in putative multimerization determinants imparted class I/II behavior in Vpr-IN complementation assays is consistent with the model that higher-order interactions are likely to be impaired by this type of (class II) IN mutation (22, 57, 58).

Other conserved CTD residues and HIV-1 replication. Although not previously ascribed specific tasks in CTD function, Arg-228, Arg-231, Lys-236, Lys-244, and Arg-263 were targeted due to their relatively high degrees of sequence conservation among HIV-1 strains (Table 1). Since HIV-1_{K236A} and HIV-1_{R231A} grew similarly to the WT (Fig. 2A), our assays failed to define an essential role for either Arg-231 or Lys-236 in HIV-1 replication. Because Lys-236 was strictly conserved among a large collection of HIV-1/SIV_{cpz} strains, it is possible that Lys-236 plays a role for the virus that lies outside the detection limits of the assays employed here. On the other hand, HIV-1_{R228A} and HIV-1_{K244A} were dead viruses (Fig. 2A and 2E) that were typed as class II mutants (Fig. 3 to 5; Table 2). Of note, Vpr-IN_{R228A} demonstrated class II mutant behavior in Vpr-IN complementation assays (Table 3).

HIV-$1_{R228A.Luc(R-)}$ and HIV-$1_{K266A.Luc(R-)}$ 2-LTR circle levels were below the limit of detection in some experiments (Fig. 3B and 4C), suggesting that Arg-228 and Lys-266 might play a role in HIV-1 nuclear localization. When expressed separately from other HIV-1 proteins, IN can localize to cell nuclei, and because of this, it has been suggested that IN might play a role in viral nuclear import (18, 34, 65, 66). Yet despite extensive effort, irrefutable evidence for a transferable nuclear localization signal within HIV-1 IN has yet to be found (4, 19, 22, 42, 48, 53, 57).

HIV-1 IN can bind to a variety of human cell proteins (27), and one, lens epithelium-derived growth factor (LEDGF) (15, 74), appears to account for IN′s karyophilic properties. This conclusion is based on findings that either RNA interference-mediated knockdown of LEDGF (55, 61) or expression of a nuclear localization-defective mutant of LEDGF (60) redistributed IN from the cell nucleus to the cytoplasm. The CTD, however, directed the nuclear accumulation of a green fluorescent fusion protein in an apparently LEDGF independent manner (61), and a Lys-rich region within the CTD of feline immunodeficiency virus IN that aligns with Arg-228 in HIV-1 (11) contributed to the karyophilic properties of a feline immunodeficiency virus IN fusion protein (83). To investigate the potential roles of Arg-228 and Lys-266 in HIV-1 nuclear localization in nondividing cells, MDM were infected with VSV-G-pseudotyped viruses. Since each mutant virus converted a normal fraction of its cDNA to 2-LTR circles (Fig. 4E and F), neither residue appeared to play an important role in nuclear import under this condition.

HIV-1_{E246K} and polyprotein processing. Mutations in IN can affect the relatively late steps of HIV-1 assembly and release (2, 7, 30, 70). The E246K change reduced HIV-1 release to approximately 5% of WT release, significantly less than that of the previously analyzed class II deletion mutant HIV-$1_{1–212}$ (Fig. 5A). Consistent with previous observations, Gag processing intermediates p41 and p25 were more readily detected in HIV-$1_{1–212}$-expressing cells than in WT-expressing cells (Fig. 6A). Two lines of evidence, however, indicated that the E246K change impacted late events differently from previously described IN deletion mutants. The first was an overall reduction in levels of $Pr55^{gag}$ processing (Fig. 6A, lanes 3, 5, and 7). The second was the failure of the protease inhibitor saquinavir to rescue release from HIV-1_{E246K}-expressing cells (Fig. 6B, lane 8). Despite the inability to support spread in infected Jurkat cell cultures (Fig. 2B), HIV-$1_{E246K.Luc(R-)}$ supported approximately 8% of the level of WT HIV-$1_{NLX.Luc(R-)}$ transduction activity (Table 2). HIV-$1_{K236A/E246A}$ (Fig. 2D) and HIV-1_{R269A} (Fig. 2E) supported weak but detectable levels of virus spread, and HIV-$1_{K236A/E246A.Luc(R-)}$ and HIV-$1_{R269A.Luc(R-)}$ transduced cells at approximately 4.0% and 11.5% of the WT level, respectively (Table 2). Based on this, we concluded that E246K was the first example of an IN mutation where a late-stage processing defect contributed significantly to the inability of the mutant virus to support multiple rounds of replication. This observation is in line with the hypothesis that antiviral drugs targeted against IN might inhibit HIV-1 replication without necessarily inhibiting the catalytic function of the DNA recombinase (57, 85).

ACKNOWLEDGMENTS

We thank J. Kappes for the pRL2P-Vpr-IN expression vector and the NIH AIDS Research and Reference Reagent Program for saquinavir.

This work was supported by NIH grants AI39394, AI52014 (to A.E.), and AI28691 (to the Dana-Farber Cancer Institute Center for AIDS Research).

REFERENCES

1. **Andrake, M. D., and A. M. Skalka.** 1995. Multimerization determinants reside in both the catalytic core and C terminus of avian sarcoma virus integrase. J. Biol. Chem. **270:**29299–29306.
2. **Ansari-Lari, M. A., L. A. Donehower, and R. Gibbs.** 1995. Analysis of human immunodeficiency virus type 1 integrase mutants. Virology **211:**332–335.
3. **Appa, R. S., C.-G. Shin, P. Lee, and S. A. Chow.** 2001. Role of the nonspecific DNA-binding region and alpha helices within the core domain of retroviral integrase in selecting target DNA sites for integration. J. Biol. Chem. **276:** 45848–45855.
4. **Armon-Omer, A., A. Graessmann, and A. Loyter.** 2004. A synthetic peptide bearing the HIV-1 integrase 161–173 amino acid residues mediates active nuclear import and binding to importin alpha: characterization of a functional nuclear localization signal. J. Mol. Biol. **336:**1117–1128.
5. **Bouyac-Bertoia, M., J. D. Dvorin, R. A. M. Fouchier, Y. Jenkins, B. E. Meyer, L. I. Wu, M. Emerman, and M. H. Malim.** 2001. HIV-1 infection requires a functional integrase NLS. Mol. Cell **7:**1025–1035.
6. **Brown, H. E. V., H. Chen, and A. Engelman.** 1999. Structure-based mutagenesis of the human immunodeficiency virus type 1 DNA attachment site: effects on integration and cDNA synthesis. J. Virol. **73:**9011–9020.
7. **Bukovsky, A., and H. Göttlinger.** 1996. Lack of integrase can markedly affect human immunodeficiency virus type 1 particle production in the presence of an active viral protease. J. Virol. **70:**6820–6825.
8. **Burke, C. J., G. Sanyal, M. W. Bruner, J. A. Ryan, R. L. LaFemina, H. L. Robbins, A. S. Zeft, C. R. Middaugh, and M. G. Cordingley.** 1992. Structural implications of spectroscopic characterization of a putative zinc finger peptide from HIV-1 integrase. J. Biol. Chem. **267:**9639–9644.
9. **Bushman, F. D., A. Engelman, I. Palmer, P. Wingfield, and R. Craigie.** 1993. Domains of the integrase protein of human immunodeficiency virus type 1 responsible for polynucleotidyl transfer and zinc binding. Proc. Natl. Acad. Sci. USA **90:**3428–3432.
10. **Cai, M., R. Zheng, M. Caffrey, R. Craigie, G. M. Clore, and A. M. Gronenborn.** 1997. Solution structure of the N-terminal zinc binding domain of HIV-1 integrase. Nat. Struct. Biol. **4:**567–577.
11. **Cannon, P. M., E. D. Byles, S. M. Kingsman, and A. J. Kingsman.** 1996. Conserved sequences in the carboxyl terminus of integrase that are essential for human immunodeficiency virus type 1 replication. J. Virol. **70:**651–657.
12. **Chen, H., and A. Engelman.** 2001. Asymmetric processing of human immunodeficiency virus type 1 cDNA in vivo: implications for functional end coupling during the chemical steps of DNA transposition. Mol. Cell. Biol. **21:**6758–6767.
13. **Chen, H., S.-Q. Wei, and A. Engelman.** 1999. Multiple integrase functions are required to form the native structure of the human immunodeficiency virus type I intasome. J. Biol. Chem. **274:**17358–17364.
14. **Chen, J. C.-H., J. Krucinski, L. J. W. Miercke, J. S. Finer-Moore, A. H. Tang, A. D. Leavitt, and R. M. Stroud.** 2000. Crystal structure of the HIV-1

integrase catalytic core and C-terminal domains: a model for viral DNA binding. Proc. Natl. Acad. Sci. USA **97:**8233–8238.
15. **Cherepanov, P., G. Maertens, P. Proost, B. Devreese, J. Van Beeumen, Y. Engelborghs, E. De Clercq, and Z. Debyser.** 2003. HIV-1 integrase forms stable tetramers and associates with LEDGF/p75 protein in human cells. J. Biol. Chem. **278:**372–381.
16. **Craigie, R.** 2002. Retroviral DNA integration, p. 613–630. *In* N. L. Craig, R. Craigie, M. Gellert, and A. M. Lambowitz (ed.), Mobile DNA II. ASM Press, Washington, D.C.
17. **DeLano, W. L.** 2002, posting date. The PyMOL molecular graphics system. [Online.] http://www.pymol.org.
18. **Depienne, C., P. Roques, C. Creminon, L. Fritsch, R. Casseron, D. Dormont, C. Dargemont, and S. Benichou.** 2000. Cellular distribution and karyophilic properties of matrix, integrase, and Vpr proteins from the human and simian immunodeficiency viruses. Exp. Cell Res. **260:**387–395.
19. **Devroe, E., A. Engelman, and P. A. Silver.** 2003. Intracellular transport of human immunodeficiency virus type 1 integrase. J. Cell Sci. **116:**4401–4408.
20. **Dirac, A. M. G., and J. Kjems.** 2001. Mapping DNA-binding sites of HIV-1 integrase by protein footprinting. Eur. J. Biochem. **268:**743–751.
21. **Drelich, M., R. Wilhelm, and J. Mous.** 1992. Identification of amino acid residues critical for endonuclease and integration activities of HIV-1 IN protein in vitro. Virology **188:**459–468.
22. **Dvorin, J. D., P. Bell, G. G. Maul, M. Yamashita, M. Emerman, and M. H. Malim.** 2002. Reassessment of the roles of integrase and the central DNA flap in human immunodeficiency virus type 1 nuclear import. J. Virol. **76:** 12087–12096.
23. **Dyda, F., A. B. Hickman, T. M. Jenkins, A. Engelman, R. Craigie, and D. R. Davies.** 1994. Crystal structure of the catalytic domain of HIV-1 integrase: similarity to other polynucleotidyl transferases. Science **266:**1981–1986.
24. **Eijkelenboom, A. P., F. M. van den Ent, A. Vos, J. F. Doreleijers, K. Hard, T. D. Tullius, R. H. Plasterk, R. Kaptein, and R. Boelens.** 1997. The solution structure of the amino-terminal HHCC domain of HIV-2 integrase: a three-helix bundle stabilized by zinc. Curr. Biol. **7:**739–746.
25. **Eijkelenboom, A. P. A. M., R. A. Puras Lutzke, R. Boelens, R. H. A. Plasterk, R. Kaptein, and K. Hård.** 1995. The DNA-binding domain of HIV-1 integrase has an SH3-like fold. Nat. Struct. Biol. **2:**807–810.
26. **Engelman, A.** 1999. In vivo analysis of retroviral integrase structure and function. Adv. Virus Res. **52:**411–426.
27. **Engelman, A.** 2003. The roles of cellular factors in retroviral integration. Curr. Top. Microbiol. Immunol. **281:**209–238.
28. **Engelman, A., F. D. Bushman, and R. Craigie.** 1993. Identification of discrete functional domains of HIV-1 integrase and their organization within an active multimeric complex. EMBO J. **12:**3269–3275.
29. **Engelman, A., and R. Craigie.** 1992. Identification of conserved amino acid residues critical for human immunodeficiency virus type 1 integrase function in vitro. J. Virol. **66:**6361–6369.
30. **Engelman, A., G. Englund, J. M. Orenstein, M. A. Martin, and R. Craigie.** 1995. Multiple effects of mutations in human immunodeficiency virus type 1 integrase on viral replication. J. Virol. **69:**2729–2736.
31. **Engelman, A., A. B. Hickman, and R. Craigie.** 1994. The core and carboxyl-terminal domains of the integrase protein of human immunodeficiency virus type 1 each contribute to nonspecific DNA binding. J. Virol. **68:**5911–5917.
32. **Esposito, D., and R. Craigie.** 1998. Sequence specificity of viral end DNA binding by HIV-1 integrase reveals critical regions for protein-DNA interaction. EMBO J. **17:**5832–5843.
33. **Fletcher, T. M., III, M. A. Soares, S. McPhearson, H. Hui, M. Wiskerchen, M. A. Muesing, G. M. Shaw, A. D. Leavitt, J. D. Boeke, and B. H. Hahn.** 1997. Complementation of integrase function in HIV-1 virions. EMBO J. **16:**5123–5138.
34. **Gallay, P., T. Hope, D. Chin, and D. Trono.** 1997. HIV-1 infection of nondividing cells through the recognition of integrase by the importin/karyopherin pathway. Proc. Natl. Acad. Sci. USA **94:**9825–9830.
35. **Gao, K., S. L. Butler, and F. Bushman.** 2001. Human immunodeficiency virus type 1 integrase: arrangement of protein domains in active cDNA complexes. EMBO J. **20:**3565–3576.
36. **Gerton, J. L., and P. O. Brown.** 1997. The core domain of HIV-1 integrase recognizes key features of its DNA substrates. J. Biol. Chem. **272:**25809–25815.
37. **Gerton, J. L., S. Ohgi, M. Olsen, J. DeRisi, and P. O. Brown.** 1998. Effects of mutations in residues near the active site of human immunodeficiency virus type 1 integrase on specific enzyme-substrate interactions. J. Virol. **72**:5046–5055.
38. **Goff, S. P.** 2001. *Retroviridae*: the retroviruses and their replication, p. 1871–1939. *In* D. M. Knipe, P. M. Howley, D. E. Griffin, R. A. Lamb, M. A. Martin, B. Roizman, and S. E. Straus (ed.), Fields virology, 4th ed. Lippincott Williams & Wilkins, Philadelphia, Pa.
39. **Harper, A. L., L. M. Skinner, M. Sudol, and M. Katzman.** 2001. Use of patient-derived human immunodeficiency virus type 1 integrases to identify a protein residue that affects target site selection. J. Virol. **75:**7756–7762.
40. **Hehl, E. A., P. Joshi, G. V. Kalpana, and V. R. Prasad.** 2004. Interaction between human immunodeficiency virus type 1 reverse transcriptase and integrase proteins. J. Virol. **78:**5056–5067.
41. **Heuer, T. S., and P. O. Brown.** 1997. Mapping features of HIV-1 integrase near selected sites on viral and target DNA molecules in an active enzyme-DNA complex by photo-cross-linking. Biochemistry **36:**10655–10665.
42. **Ikeda, T., H. Nishitsuji, X. Zhou, N. Nara, T. Ohashi, M. Kannagi, and T. Masuda.** 2004. Evaluation of the functional involvement of human immunodeficiency virus type 1 integrase in nuclear import of viral cDNA during acute infection. J. Virol. **78:**11563–11573.
43. **Jenkins, T. M., A. Engelman, R. Ghirlando, and R. Craigie.** 1996. A soluble active mutant of HIV-1 integrase: involvement of both the core and the C-terminal domains in multimerization. J. Biol. Chem. **271:**7712–7718.
44. **Jenkins, T. M., D. Esposito, A. Engelman, and R. Craigie.** 1997. Critical contacts between HIV-1 integrase and viral DNA identified by structure-based analysis and photo-crosslinking. EMBO J. **16:**6849–6859.
45. **Kalpana, G. V., A. Reicin, G. S. W. Cheng, M. Sorin, S. Paik, and S. P. Goff.** 1999. Isolation and characterization of an oligomerization-negative mutant of HIV-1 integrase. Virology **259:**274–285.
46. **Kim, S. Y., R. Byrn, J. Groopman, and D. Baltimore.** 1989. Temporal aspects of DNA and RNA synthesis during human immunodeficiency virus infection: evidence for differential gene expression. J. Virol. **63:**3708–3713.
47. **Kuiken, C. L., B. Foley, E. O. Freed, B. Hahn, B. Korber, P. A. Marx, F. McCutchan, J. W. Mellors, and S. Wolinsky.** 2002. HIV sequence compendium 2002, report no. LA-UR 03-3564. Theoretical Biology and Biophysics Group, Los Alamos National Laboratory, Los Alamos, N. Mex.
48. **Kukolj, G., K. Jones, and A. Skalka.** 1997. Subcellular localization of avian sarcoma virus and human immunodeficiency virus type 1 integrases. J. Virol. **71:**843–847.
49. **Kulkosky, J., K. S. Jones, R. A. Katz, J. P. Mack, and A. M. Skalka.** 1992. Residues critical for retroviral integrative recombination in a region that is highly conserved among retroviral/retrotransposon integrases and bacterial insertion sequence transposases. Mol. Cell. Biol. **12:**2331–2338.
50. **Leavitt, A. D., G. Robles, N. Alesandro, and H. E. Varmus.** 1996. Human immunodeficiency virus type 1 integrase mutants retain in vitro integrase activity yet fail to integrate viral DNA efficiently during infection. J. Virol. **70:**721–728.
51. **Leavitt, A. D., L. Shiue, and H. E. Varmus.** 1993. Site-directed mutagenesis of HIV-1 integrase demonstrates differential effects on integrase functions in vitro. J. Biol. Chem. **268:**2113–2119.
52. **Lee, S. P., J. Xiao, J. R. Knutson, M. S. Lewis, and M. K. Han.** 1997. Zn^{2+} promotes the self-association of human immunodeficiency virus type-1 integrase in vitro. Biochemistry **36:**173–180.
53. **Limón, A., E. Devroe, R. Lu, H. Z. Ghory, P. A. Silver, and A. Engelman.** 2002. Nuclear localization of human immunodeficiency virus type 1 preintegration complexes (PICs): V165A and R166A are pleiotropic integrase mutants primarily defective for integration, not PIC nuclear import. J. Virol. **76:**10598–10607.
54. **Limón, A., N. Nakajima, R. Lu, H. Z. Ghory, and A. Engelman.** 2002. Wild-type levels of nuclear localization and human immunodeficiency virus type 1 replication in the absence of the central DNA flap. J. Virol. **76:**12078–12086.
55. **Llano, M., M. Vanegas, O. Fregoso, D. Saenz, S. Chung, M. Peretz, and E. M. Poeschla.** 2004. LEDGF/p75 determines cellular trafficking of diverse lentiviral but not murine oncoretroviral integrase proteins and is a component of functional lentiviral preintegration complexes. J. Virol. **78:**9524–9537.
56. **Lodi, P. J., J. A. Ernst, J. Kuszewski, A. B. Hickman, A. Engelman, R. Craigie, G. M. Clore, and A. M. Gronenborn.** 1995. Solution structure of the DNA binding domain of HIV-1 integrase. Biochemistry **34:**9826–9833.
57. **Lu, R., A. Limón, E. Devroe, P. A. Silver, and A. Engelman.** 2004. Class II integrase mutants with changes in putative nuclear localization signals are primarily blocked at a post-nuclear entry step of human immunodeficiency virus type 1 replication. J. Virol. **78:**12735–12746.
58. **Lu, R., A. Limón, H. Z. Ghory, and A. Engelman.** 2005. Genetic analyses of DNA-binding mutants in the catalytic core domain of human immunodeficiency virus type 1 integrase. J. Virol. **79:**2493–2505.
59. **Lu, R., N. Nakajima, W. Hofmann, M. Benkirane, K.-T. Jeang, J. Sodroski, and A. Engelman.** 2004. Simian virus 40-based replication of catalytically inactive human immunodeficiency virus type 1 integrase mutants in nonpermissive T cells and monocyte-derived macrophages. J. Virol. **78:**658–668.
60. **Maertens, G., P. Cherepanov, Z. Debyser, Y. Engelborghs, and A. Engelman.** 2004. Identification and characterization of a functional nuclear localization signal in the HIV-1 integrase interactor LEDGF/p75. J. Biol. Chem. **279:** 33421–33429.
61. **Maertens, G., P. Cherepanov, W. Pluymers, K. Busschots, E. De Clercq, Z. Debyser, and Y. Engelborghs.** 2003. LEDGF/p75 is essential for nuclear and chromosomal targeting of HIV-1 integrase in human cells. J. Biol. Chem. **278:**33528–33539.
62. **Mumm, S. R., and D. P. Grandgenett.** 1991. Defining nucleic acid-binding properties of avian retrovirus integrase by deletion analysis. J. Virol. **65:** 1160–1167.
63. **Nakajima, N., R. Lu, and A. Engelman.** 2001. Human immunodeficiency virus type 1 replication in the absence of integrase-mediated DNA recom-

bination: definition of permissive and nonpermissive T-cell lines. J. Virol. **75:**7944–7955.
64. **Petit, C., O. Schwartz, and F. Mammano.** 2000. The karyophilic properties of human immunodeficiency virus type 1 integrase are not required for nuclear import of proviral DNA. J. Virol. **74:**7119–7126.
65. **Petit, C., O. Schwartz, and F. Mammano.** 1999. Oligomerization within virions and subcellular localization of human immunodeficiency virus type 1 integrase. J. Virol. **73:**5079–5088.
66. **Pluymers, W., P. Cherepanov, D. Schols, E. De Clercq, and Z. Debyser.** 1999. Nuclear localization of human immunodeficiency virus type 1 integrase expressed as a fusion protein with green fluorescent protein. Virology **258:**327–332.
67. **Priet, S., J.-M. Navarro, G. Querat, and J. Sire.** 2003. Reversion of the lethal phenotype of an HIV-1 integrase mutant virus by overexpression of the same integrase mutant protein. J. Biol. Chem. **278:**20724–20730.
68. **Puras Lutzke, R. A., and R. H. A. Plasterk.** 1998. Structure-based mutational analysis of the C-terminal DNA-binding domain of human immunodeficiency virus type 1 integrase: critical residues for protein oligomerization and DNA binding. J. Virol. **72:**4841–4848.
69. **Puras Lutzke, R. A., C. Vink, and R. H. A. Plasterk.** 1994. Characterization of the minimal DNA-binding domain of the HIV integrase protein. Nucleic Acids Res. **22:**4125–4131.
70. **Quillent, C., A. M. Borman, S. Paulous, C. Dauguet, and F. Clavel.** 1996. Extensive regions of pol are required for efficient human immunodeficiency virus polyprotein processing and particle maturation. Virology **219:**29–36.
71. **Rice, P. A., and T. A. Baker.** 2001. Comparative architecture of transposase and integrase complexes. Nat. Struct. Biol. **8:**302–307.
72. **Shibagaki, Y., and S. A. Chow.** 1997. Central core domain of retroviral integrase is responsible for target site selection. J. Biol. Chem. **272:**8361–8369.
73. **Stevenson, M.** 2002. Molecular biology of lentivirus-mediated gene transfer. Curr. Top. Microbiol. Immunol. **261:**1–30.
74. **Turlure, F., E. Devroe, P. A. Silver, and A. Engelman.** 2004. Human cell proteins and human immunodeficiency virus DNA integration. Front. Biosci. **9:**3187–3208.
75. **van den Ent, F. M. I., A. Vos, and R. H. A. Plasterk.** 1998. Mutational scan of the human immunodeficiency virus type 2 integrase protein. J. Virol. **72:**3916–3924.
76. **van Gent, D. C., A. A. M. O. Groeneger, and R. H. A. Plasterk.** 1992. Mutational analysis of the integrase protein of human immunodeficiency virus type 2. Proc. Natl. Acad. Sci. USA **89:**9598–9602.
77. **van Gent, D. C., C. Vink, A. A. M. O. Groeneger, and R. H. A. Plasterk.** 1993. Complementation between HIV integrase proteins mutated in different domains. EMBO J. **12:**3261–3267.
78. **Vink, C., A. M. Oude Groeneger, and R. H. A. Plasterk.** 1993. Identification of the catalytic and DNA-binding region of the human immunodeficiency virus type I integrase protein. Nucleic Acids Res. **21:**1419–1425.
79. **Wang, J.-Y., H. Ling, W. Yang, and R. Craigie.** 2001. Structure of a two-domain fragment of HIV-1 integrase: implications for domain organization in the intact protein. EMBO J. **20:**7333–7343.
80. **Wiskerchen, M., and M. A. Muesing.** 1995. Human immunodeficiency virus type 1 integrase: effects of mutations on viral ability to integrate, direct viral gene expression from unintegrated viral DNA templates, and sustain viral propagation in primary cells. J. Virol. **69:**376–386.
81. **Woerner, A. M., M. Klutch, J. G. Levin, and C. J. Marcus-Sekura.** 1992. Localization of DNA binding activity of HIV-1 integrase to the C-terminal half of the protein. AIDS Res. Hum. Retrovir. **8:**297–304.
82. **Woerner, A. M., and C. J. Marcus-Sekura.** 1993. Characterization of a DNA binding domain in the C-terminus of HIV-1 integrase by deletion mutagenesis. Nucleic Acids Res. **21:**3507–3511.
83. **Woodward, C. L., Y. Wang, W. J. Dixon, H. Htun, and S. A. Chow.** 2003. Subcellular localization of feline immunodeficiency virus integrase and mapping of its karyophilic determinant. J. Virol. **77:**4516–4527.
84. **Wu, X., H. Liu, H. Xiao, J. A. Conway, E. Hunter, and J. C. Kappes.** 1997. Functional RT and IN incorporated into HIV-1 particles independently of the Gag/Pol precursor protein. EMBO J. **16:**5113–5122.
85. **Yung, E., M. Sorin, E.-J. Wang, S. Perumal, D. Ott, and G. V. Kalpana.** 2004. Specificity of interaction of INI1/hSNF5 with retroviral integrases and its functional significance. J. Virol. **78:**2222–2231.
86. **Zheng, R., T. M. Jenkins, and R. Craigie.** 1996. Zinc folds the N-terminal domain of HIV-1 integrase, promotes multimerization, and enhances catalytic activity. Proc. Natl. Acad. Sci. USA **93:**13659–13664.
87. **Zhu, K., C. Dobard, and S. A. Chow.** 2004. Requirement for integrase during reverse transcription of human immunodeficiency virus type 1 and the effect of cysteine mutations of integrase on its interactions with reverse transcriptase. J. Virol. **78:**5045–5055.